URN (Paper): urn:nbn:de:gbv:ilm1-2014iwk-061:2

58th ILMENAU SCIENTIFIC COLLOQUIUM
Technische Universität Ilmenau, 08 – 12 September 2014
URN: urn:nbn:de:gbv:ilm1-2014iwk:3

INVESTIGATIONS ON THE DAMPING PROPERTIES OF VACUUM-COMPATIBLE AEROSTATIC JOURNAL GAS BEARING ELEMENTS

Nils Heidler [1,2], Tobias Holub [1], Stefan Risse [1], Ramona Eberhardt [1]

[1]Fraunhofer Institute for Applied Optics and Precision Engineering IOF, Jena, Germany;
[2]Institute of Applied Physics, Friedrich-Schiller-University, Jena, Germany

ABSTRACT

Gas bearing elements with special sealing units can be used to realize high-precise movements within a vacuum environment. During the transmission of the surrounding pressure of the bearing from normal atmosphere to vacuum, the properties of the bearing change.
Within this paper, the changes of the bearings damping parameters are investigated. An experimental setup is used to excite an aerostatic journal gas bearing and measure the resulting system response of the element. The system response is used to obtain the damping constant and the eigen angular frequency. For small deflection amplitudes close to the concentric position of bushing and cylinder, the investigated aerostatic journal gas bearing element shows a very strong damping behavior.

1. INTRODUCTION

For positioning processes with an accuracy in the nanometer range, the usage of gas bearing guides is beneficial, since the friction is negligible and no stick-slip effects occur.
The positive characteristics of the gas bearings are to be transferred into a vacuum environment, because positioning systems in the semiconductor industry (e.g. for EUV or E-beam lithography) or for high-precise measurement systems have to combine a high positioning accuracy with a vacuum environment.
To restrict the leaking flow of the gas bearing into the vacuum environment, a special sealing unit is used to exhaust the supplied gas. The commonly used method uses a plurality of non-contact sealing stages. Each stage consists of one exhaustion groove and one seal gap comprising a high flow resistance. A schematic drawing of two alternative sealing unit setups is shown in Figure 1. The exhaust groove of the first stage can be connected to atmospheric pressure, resulting in a known system behavior of the gas bearings. The remaining exhaust grooves are connected to vacuum pumps to reduce the amount of gas, which is leaking through the last seal gap into the vacuum environment.
The favorable setup of this kind of sealing unit is the connection of all exhaustion grooves to external vacuum pumps [1], [2]. The advantage of this setup is the more effective exhaustion of the gas, resulting in a lower final pressure of the vacuum system or in a reduced number of sealing stages while keeping a comparable vacuum level. The disadvantageous effect is the reduced pressure at the direct surrounding of the bearing element and hence the changed pressure profile within the bearing gap. This results in a change of the parameters of the bearing element since the pressure profile is responsible for the properties of the element. These changes have to be known to enable the design and dimensioning of positioning systems using air bearing elements with this sealing unit setup [3], [4].

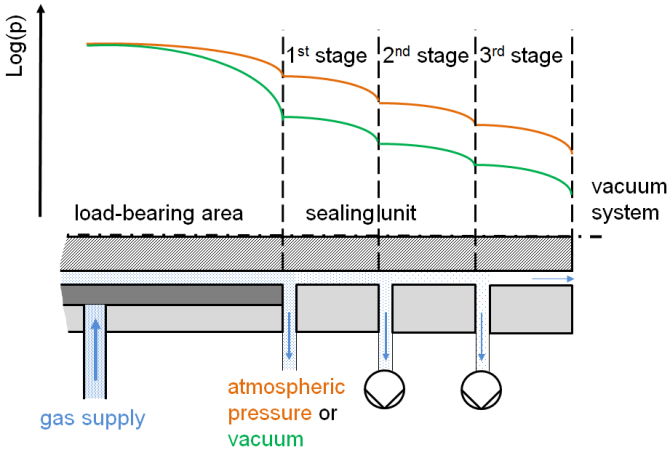

Figure 1: Schematic sectional view of gas bearing element with three stage sealing unit (not to scale)

Within this paper, the change of the damping behavior of an aerostatic journal gas bearing element during the transmission of the surrounding pressure from atmospheric pressure to vacuum is investigated.

2. ANALYTIC

The basis for the analytical description of the damping properties is the equation of motion (1) for free natural damped vibrations for one degree of freedom.

$$\ddot{z} + 2\delta\dot{z} + \omega^2 z = 0 \tag{1}$$

Here $\delta = \frac{d}{2m}$ denotes the damping constant and $\omega = \sqrt{\frac{c}{m}}$ the eigen angular frequency with the damping coefficient d, the stiffness c and the mass m of the system.
Using the exponential approach $z(t) = Ae^{\lambda t}$ the characteristic equation of the system is obtained.

$$\lambda^2 + 2\delta\lambda + \omega^2 = 0 \tag{2}$$

The solution of this equation is expressed by the following expression, using the definition of the damping ratio $D = \frac{\delta}{\omega}$.

$$\lambda_{1/2} = -\delta \pm \sqrt{\delta^2 - \omega^2} = -\delta \pm \omega\sqrt{D^2 - 1} \tag{3}$$

The damping behavior of the system depends on the root term $(D^2 - 1)$ of Equation (3). If $D > 1$, a very strong damping behavior exists. For $D \ll 1$ the system is called weakly damped and for $D < 1$ it is called strongly damped. For $D = 1$ the system is critically damped [5]. In Figure 2, exemplary system behaviors for different damping ratios are shown (zero velocity initial condition).

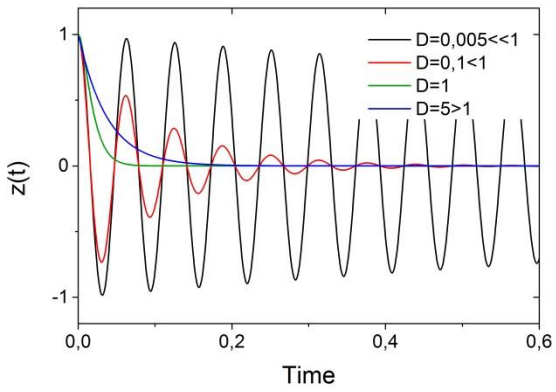

Figure 2: Exemplarily system behavior for different damping ratios D

The shown equations are valid for linear oscillations. The damping coefficient d and the stiffness c of the air bearing element are non-constant values and vary with amplitude changes due to the nonlinear oscillation behavior of the gas pressure profile within the bearing gap. According to Schroter [6], the damping constant and the eigenfrequency of plan gas bearing elements can be considered as approximately constant for small amplitudes.

3. EXPERIMENTAL SETUP

For the experimental investigation an aerostatic journal gas bearing element with a porous flow restrictor, further referred to as main bushing, is used. The tactile measured diameter of the main bushing is $40{,}046 \pm 0{,}002$ mm with a shape deviation of 4 µm. The counterpart is a ceramic cylinder with a diameter of $40{,}017 \pm 0{,}002$ mm with a shape deviation of 2 µm. The resulting concentric gap height h_0 is $14{,}5 \pm 2$ µm.

The aim of the experimental setup is to excite the system in accordance to Schroter [6] with small excitation. The resulting system response in terms of the time-resolved movement of the system will be used to obtain the damping constant and the eigen angular frequency of the system.

The designed and used experimental test rig to realize this approach is shown in Figure 3. To consider the change of the surrounding pressure p_k for the different sealing unit setups, the test rig can be operated in a vacuum chamber. The pressure in the vacuum chamber can be adapted to the pressure of the first sealing stage.

The cylinder is fixed to the setup frame. The investigated main bushing is fixed in a mount which also holds a hollow supporting cylinder whose axis is precisely orthogonal aligned in respect to the rotational axis of the journal bearing. The alignment is realized with an angle error below 0,06 mrad using a coordinate measuring machine. This supporting cylinder is the counterpart of a supporting bushing which is used to restrict the free movement of the main bushing along its two remaining degree of freedom (translation along y-axis, rotation around y-axis; coordinate system see Figure 3). The mount of the supporting bushing is frame fixed and the relative position to the main cylinder within x-direction was adjusted during the setting of the test rig. In addition, the mount has a built-in flexure hinge to account for manufacturing and alignment errors.

Within the hollow supporting cylinder, a frame fixed piezo actuator is used to deflect the main bushing. Three capacitive displacement sensors are used to detect the movement of the free oscillation into the z-direction of the system. Three additional sensors are used to be able to monitor all six degrees of freedom of the system during the movement. The evaluation of the final movement is based on the movement of the bushing center into z- direction.

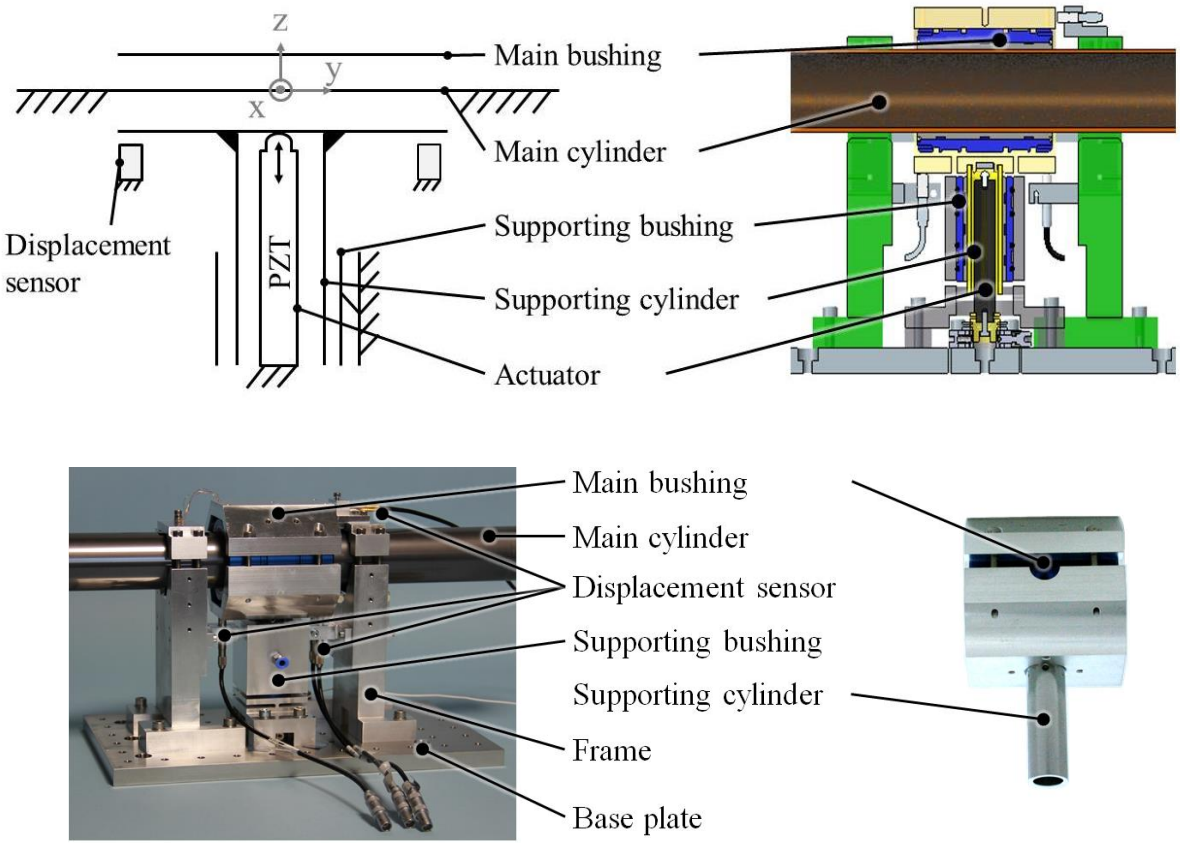

Figure 3: Experimental test rig
(top: technical principle and cross-sectional view of CAD model, bottom: picture)

The contact between the actuator and the mount of the main bushing is designed as a sphere/flat connection to realize a defined point of the force transmission. The position of this point is adjustable within x- and y- direction. During the setting of the test rig, this position is adjusted to the center of mass of the main bushing/mount system. This is done by minimizing the auxiliary movements (rotation around x- and y-axis) during the deflection of the system.
The measurement procedure is as follows. The starting state of the system is defined while the supply pressure p_s of the main bushing and the supply pressure $p_s^{support}$ of the supporting bushing are applied. In this state the main bushing is lifted to a starting gap height. Here, the only applied load is the systems dead load of 0,75 kg resulting in an eccentricity of the main bushing relative to the cylinder of approx. 0,3 µm.
From this starting position, the actuator deflects the system to the initial deflection z_a. From this position, the actuator is pulled back very quickly, to enable a free movement of the main bushing back to the starting position. To prove that the actuator is pulled back faster than the bushing moves back into the starting position, a comparison measurement of both had been carried out. The result of these measurements with matched time axes can be seen in Figure 4.

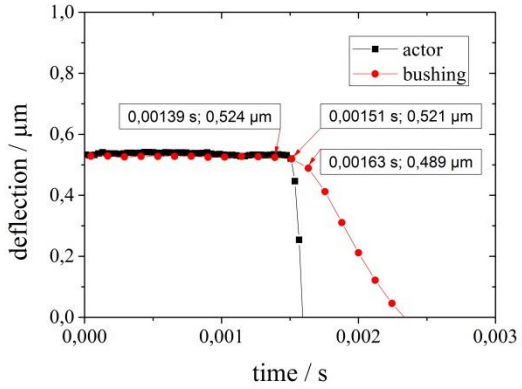

Figure 4: Movement of actuator and bushing after deflection

The acceleration of the actuator reaches a maximum of 130 m/s² while the maximum acceleration of the bushing is approx. 3 m/s².
For the evaluation of the damping parameters, the experimental obtained data has to be post-processed. The starting time of the free movement has to be known and defined as $t=0$. This is corresponding to the moment of the pull back of the actuator. The corresponding data point of the bushing movement was determined by its position change. The noise of the displacement sensor is approx. 3 nm. When the position change between two data points exceeds 5 nm, this data point is defined as $t=0$. For the exemplary measurement in Figure 4, this data point is (0,00151 s; 0,521 µm).
With the above measurement procedure, the bushing was tested with different input parameter values (see Table 1). All pressure values are absolute values. The additional values for $\boldsymbol{z_a}$ were chosen to gain more information in the range of small initial deflection amplitudes. Every parameter combination was measured ten times for statistical verification.

Table 1: Investigated input parameters

input parameter	value
p_s	300.000 Pa; 400.000 Pa; 500.000 Pa
$p_s^{support}$	200.000 Pa
p_k	100.000 Pa; 1500 Pa
z_a	0,1 µm; 0,5 µm; 1,0 µm; 2,5 µm
additional z_a for $p_s = 400$ kPa	0,05 µm; 0,2 µm; 0,3 µm; 0,4 µm;

4. RESULTS

The damping behavior of the aerostatic journal gas bearing element is shown in Figure 5 for an exemplarily measurement. The bushing starts at a deflection of $z_a = 0{,}1\ \mu m$, reaches the starting position $z = 0$, after approx. 1 ms, overshoots this position to a minimum at $z(t = 0{,}0035s) = -0{,}046\ \mu m$ and afterwards approaches the starting position asymptotically.

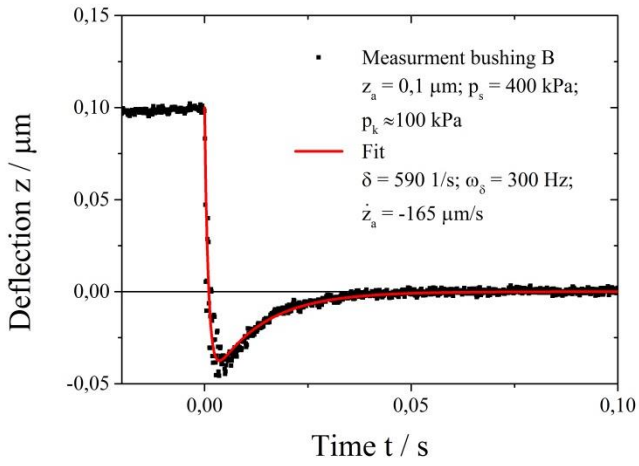

Figure 5: Exemplarily measurement of the bushing and the corresponding fitted curve

This behavior is typical for a very strong damped system with an initial velocity condition. The existence of an initial velocity of the system cannot be directly derived from the systems starting position. The system is at a rest before the actuator is pulled back (see Figure 5). The reason for the initial velocity is most likely due to the changed pressure profile within the bearing gap during the deflection of the system. The pressure in the direction of the deflection increases while the local bearing gap height decreases. After removing the additional force of the actuator, the introduced pressure difference acts on the system and realizes an impulse-like force on a very short-term time scale.
Assuming that an initial velocity $\dot{z}_a$ is present, Equation (4) can be derived based on Equation (1)-(3) and the initial conditions $z(t=0) = z_a$ and $\dot{z}(\mathrm{t}=0) = \dot{z}_a$.

$$z(t) = \frac{e^{-\delta t}\left[z_a\sqrt{\delta^2-\omega^2}\cosh\left(t\sqrt{\delta^2-\omega^2}\right) + (\dot{z}_a + z_a\delta)\sinh\left(t\sqrt{\delta^2-\omega^2}\right)\right]}{\sqrt{\delta^2-\omega^2}} \quad (4)$$

Equation (4) is used to obtain the damping parameters δ and ω as well as the initial velocity $\dot{z}_a$. This is realized by a fitting procedure that minimizes the error square values relating to the experimental data. The result of this fitting procedure is plotted against the experimental data in Figure 5.
The fitting procedure is applied to all conducted measurements. The mean value and the 2σ standard deviation of the fitted damping parameters for all investigated input parameters are shown in Figure 6 and Figure 7.

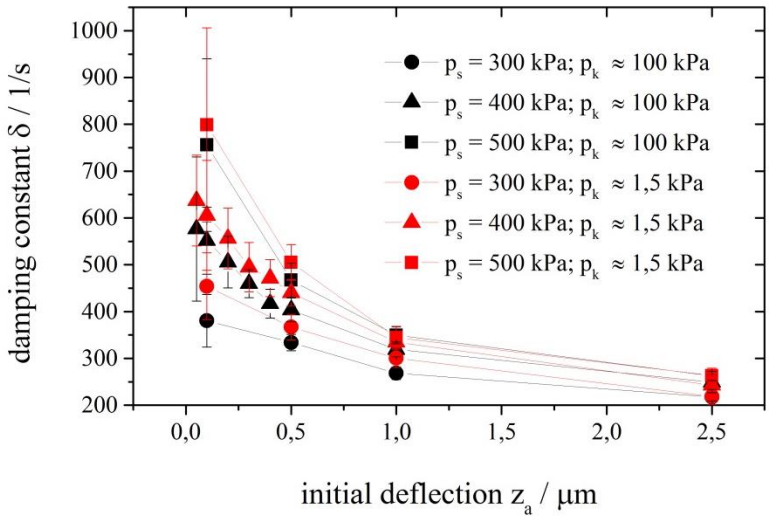

Figure 6: Damping constant over initial deflection

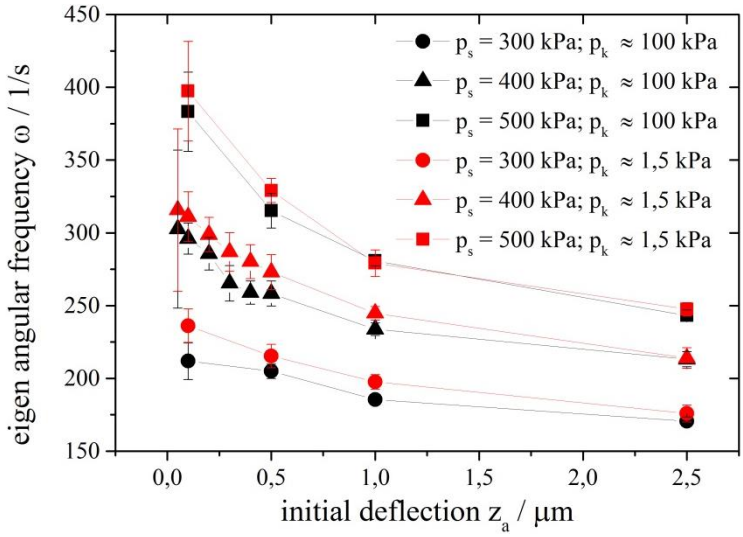

Figure 7: Eigen angular frequency over initial deflection

It can be seen, that the damping constant as well as the eigen angular frequency increase with decreasing initial deflection. Both increase also for higher supply pressures and during the transmission of the surrounding pressure from normal atmosphere to vacuum. The dependence on the supply pressure is more pronounced for ω. The standard deviations of both parameters increases significantly for initial deflections below 0,1 µm. Hence, Schroters [6] assumption of constant damping parameters at small amplitudes for plan gas bearing elements cannot be confirmed for journal gas bearing elements, since the quantitative information in this range is low.

When expressing the damping parameters in terms of the damping Ratio D, the curves in Figure 8 are obtained. The damping ratio rises with decreasing initial deflections, where the slope is higher for higher supply pressures at small deflection amplitudes. The effect of the change of the surrounding pressure on D is small and mostly within the standard deviation of the measurement.

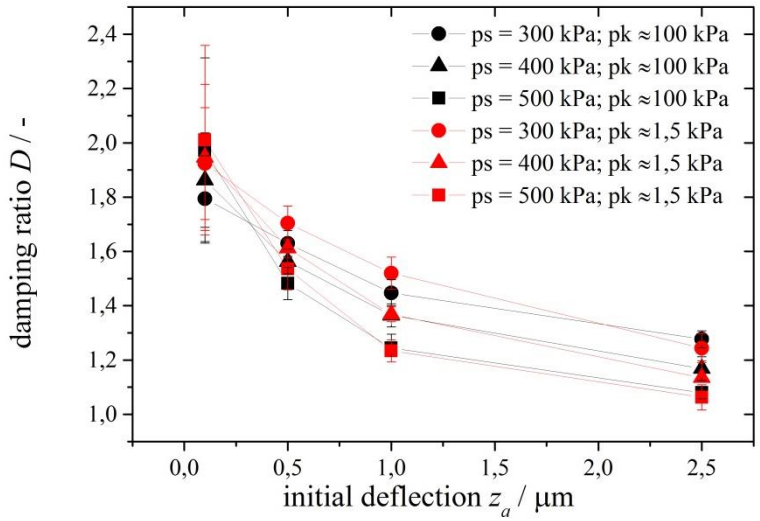

Figure 8: Damping ratio over initial deflection

Figure 9 shows the fitted values of the initial velocity. The absolute value of $\dot{z}_a$ increases with the initial deflection. For small initial deflections, the change is approximately linear. The negative sign signalizes that the direction of the velocity is contrary to the direction of the deflection. The velocity for the measurements at vacuum conditions is slightly higher than for normal atmosphere conditions. The rise of the supply pressure also results in an increased velocity.

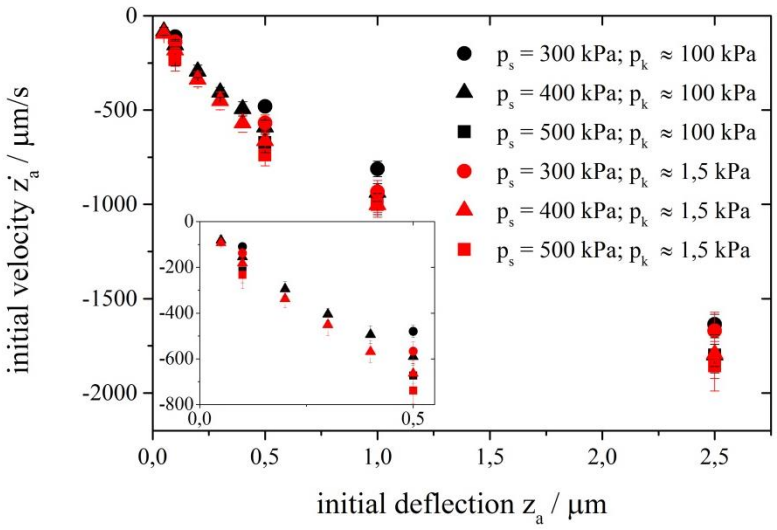

Figure 9: Initial velocity over initial deflection

The comparison of three exemplarily measurements in Figure 10 shows the difference of the time based system response for different supply pressures for $z_a = 0{,}5\ \mu m$. The minima position after the overshoot of the starting position divers by only 15 nm (3% of z_a). After 50 ms, all three signals are within a $0{,}02 \cdot z_a$ range of the starting position.

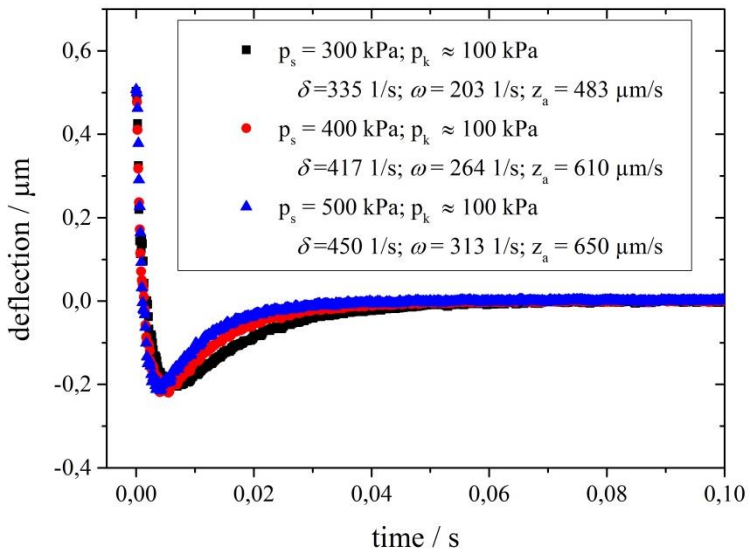

Figure 10: Comparison between exemplarily system responses for different supply pressures

5. CONCLUSION

This paper shows, that the investigated aerostatic journal gas bearing element is very strongly damped (D>1). This is tested for small deflection amplitudes close to the concentric position of bushing and cylinder. The transmission of the surrounding pressure from normal atmosphere to vacuum slightly increases the damping of the system.
The main influence on the damping is the initial deflection amplitude. For smaller deflections, the damping of the system is higher. In general, the time based system response for different supply pressures and surrounding pressures shows only narrow differences.

REFERENCES

[1] C. Schenk, S. Risse, G. Schubert et al. “Gas-lubricated guidings – suitable for vacuum systems?“ 53rd Internationales Wissenschaftliches Kolloquium, Technische Universität Ilmenau, 2008
[2] N. Heidler, C. Schenk, G. Harnisch et al. “Contact-free exhaust system for vacuum compatible gas bearing guides.” Precision Engineering, 36: 37-43, 2012
[3] C. Schenk, S. Buschmann, S. Risse et al. “Comparison between flat aerostatic gas-bearing pads with orifice and porous feedings at high-vacuum conditions.” Precision Engineering, 32: 319–328, 2008
[4] N. Heidler, T. Holub, S. Risse et al. “Load bearing capacity and stiffness of porous journal gas bearing elements in a vacuum environment” Proceedings of 26th Annual Meeting of the American Society for Precision Engineering, 2011
[5] DIN 1311 Schwingungen und schwingungsfähige Systeme Teil 2, 08/2002. Deutsches Institut für Normung e.V.
[6] A. Schroter, “Ausgleichsvorgänge und Strömungsgeräusche bei aerostatischen Lagern mit flächig verteilten Mikrodüsen“ Fortschrittsberichte VDI, Reihe 1 Nr. 245, VDI-Verlag Düsseldorf, 1995

CONTACTS

Dipl.-Ing.(FH) Nils Heidler Nils.Heidler@iof.fraunhofer.de